Shell-model Monte Carlo studies of neutron-rich nuclei in the $1s$-$0d$-$1p$-$0f$ shells

D. J. Dean,[1] M. T. Ressell,[2,4] M. Hjorth-Jensen,[3] S. E. Koonin,[2] K. Langanke,[5] and A. P. Zuker[6]
[1]*Physics Division, Oak Ridge National Laboratory, P.O. Box 2008, Oak Ridge, Tennessee 37831 and Department of Physics and Astronomy, University of Tennessee, Knoxville, Tennesseek 37996*
[2]*W.K. Kellogg Radiation Laboratory, 106-38, California Institute of Technology, Pasadena, California 91125*
[3]*Nordita, Blegdamsvej 17, DK-2100 Copenhagen Ø, Denmark and Department of Physics, University of Oslo, Norway*
[4]*Astronomy and Astrophysics Center, University of Chicago, 5640 South Ellis Avenue, Chicago, Illinois 60637*
[5]*Institute for Physics and Astronomy, Aarhus University, Denmark*
[6]*Institut de Recherches Subatomiques, Bâtiment 27, IN2P3-CNRS/Université Louis Pasteur Boîte Postal 28, F-67037 Strasbourg Cedex 2, France*
(Received 16 November 1998)

We demonstrate the feasibility of realistic shell-model Monte Carlo (SMMC) calculations spanning multiple major shells, using a realistic interaction whose bad saturation and shell properties have been corrected by a newly developed general prescription. Particular attention is paid to the approximate restoration of translational invariance. The model space consists of the full sd-pf shells. We include in the study some well-known $T=0$ nuclei and several unstable neutron-rich ones around $N=20,28$. The results indicate that SMMC calculations can reproduce binding energies, $B(E2)$ transitions, and other observables with an interaction that is practically parameter free. Some interesting insight is gained into the nature of deep correlations. The validity of previous studies is confirmed. [S0556-2813(99)00405-7]

PACS number(s): 21.60.Cs, 21.60.Ka, 27.40.+z, 21.10.Dr

I. INTRODUCTION

Studies of extremely neutron-rich nuclei have revealed a number of intriguing new phenomena. Two sets of these nuclei that have received particular attention are those with neutron number N in the vicinity of $1s0d$ and $0f_{7/2}$ shell closures ($N\approx 20$ and $N\approx 28$). Experimental studies of neutron-rich Mg and Na isotopes indicate the onset of deformation, as well as the modification of the $N=20$ shell gap for ^{32}Mg and nearby nuclei [1]. Inspired by the rich set of phenomena occurring near the $N=20$ shell closure when $N \gg Z$, attention has been directed to nuclei near the $N=28$ (sub)shell closure for a number of S and Ar isotopes [2,3] where similar, but less dramatic, effects have been seen as well.

In parallel with the experimental efforts, there have been several theoretical studies seeking to understand and, in some cases, predict properties of these unstable nuclei. Both mean-field [4,5] and shell-model calculations [2,3,6–10] have been proposed. The latter require a severe truncation to achieve tractable model spaces, since the successful description of these nuclei involves active nucleons in both the sd and the pf shells. The natural basis for the problem is therefore the full sd-pf space, which puts it out of reach of exact diagonalization on current hardware.

Shell-model Monte Carlo (SMMC) methods [11–13] offer an alternative to direct diagonalization when the bases become very large. Though SMMC methods provide limited detailed spectroscopic information, they can predict, with good accuracy, overall nuclear properties such as masses, total strengths, strength distributions, and deformation — precisely those quantities probed by recent experiments. It thus seems natural to apply SMMC methods to these unstable neutron-rich nuclei. Two questions will arise — center-of-mass motion and choice of the interaction — that are not exactly new, but demand special treatment in very large spaces.

The center-of-mass problem concerns momentum conservation. It was investigated for the first time by Elliott and Skyrme in 1955 [14], and a vast literature on the subject has developed, but as of now, the methods proposed have not managed to reconcile rigor and applicability. Section II will be devoted to explaining why this is so and to describe how — short of ensuring exact momentum conservation — it is possible within a SMMC context to assess the damage and control it in order to perform meaningful calculations.

There has long been a consensus that G matrices derived from potentials consistent with NN data [15] are the natural shell-model choice. Unfortunately, such interactions give results that rapidly deteriorate as the number of particles increases. Two alternative cures have been proposed: sets of fitted matrix elements (all the shell-model work quoted above) or minimal ''monopole'' modifications [16]. The latter restricts the fit to far fewer quantities: some average matrix elements, which are the ones that suffer from the bad saturation and shell properties of the realistic potentials. Both approaches have the common shortcoming of needing data to determine the fitted numbers, but recently a general parametrization of the monopole field (H_m) has become available that could be used to replace the G-matrix centroids for any model space [17]. The interaction we present in Sec. III is the first monopole modified G matrix free of parameters other than the six entering the independently derived H_m.

Section IV contains results for a number of unstable, neutron-rich nuclei near the $N=20$ and 28 shell closures and compares them to experiment and to other truncated shell-model calculations. Section V is devoted to a discussion of what we have accomplished and surveys further applications of such calculations.

II. SMMC AND CENTER-OF-MASS MOTION

By momentum conservation, a many-body wave function must factorize as $\Psi(\mathbf{r})=\phi(R)\Psi(\mathbf{r}_{\rm rel})$, where R is the center-of-mass coordinate and $\mathbf{r}_{\rm rel}$ the relative ones. There are formalisms in which the latter are constructed explicitly, but they lead to very hard problems of antisymmetrization. What can be done in a shell-model context is to work with a basis that ensures that the eigenstates automatically factorize as requested. This is accomplished by taking $\phi(R)$ to be a harmonic oscillator state, which implies that the basis must produce eigenstates of

$$H_{\rm c.m.}=\frac{\tilde{P}^2}{2Am}+\frac{1}{2}mA\omega^2\tilde{R}^2-\frac{3}{2}\hbar\omega, \tag{1}$$

with $\tilde{P}=\Sigma_{i=1,A}p_i$, and $\tilde{R}=(\Sigma_{i=1,A}r_i)/A$.

In order to diagonalize this one-body Hamiltonian in the SM basis, we have to rewrite it using

$$\left(\sum_{i=1}^{A}p_i\right)^2=A\sum_{i=1}^{A}p_i^2-\sum_{i<j}(p_i-p_j)^2, \tag{2}$$

along with a similar expression for the coordinates. Then $H_{\rm c.m.}=h_1+h_2$, where h_1 is a one-body oscillator spectrum, and h_2 an oscillator two-body force. If one considers the matrix element $\langle n_1l_1n_2l_2|h_2|n_3l_3n_4l_4\rangle$, it is quite easy to convince oneself — using a general property of the Talmi-Moshinsky transformation and the oscillator form of h_2 — that $2n_1+l_1+2n_2+l_2=2n_3+l_3+2n_4+l_4$. In other words, $H_{\rm c.m.}$ conserves the number of oscillator quanta. This implies that if a basis contains *all* states of (or up to) $n\hbar\omega$ excitations, diagonalizing a translationally invariant Hamiltonian would ensure the factorization of the center-of-mass wave function. To separate the wave functions with $0\hbar\omega$ center-of-mass quanta it would be sufficient to do the calculations with

$$\tilde{H}=H+\beta_{\rm c.m.}H_{\rm c.m.}, \tag{3}$$

choosing a large $\beta_{\rm c.m.}$ (not to be confused with the SMMC inverse temperature). Thus, the procedure to deal with the center-of-mass problem is conceptually straightforward. Practically, things are not so simple. In ^{32}Mg, for example, the sd-pf basis will contain states having between 0 and 16 $\hbar\omega$ quanta; however, it is very far from containing them all, and it does not even contain all those of 1 $\hbar\omega$. Then — and this point is crucial — the restriction of $H_{\rm c.m.}$ to the basis *is no longer* $H_{\rm c.m.}$. As a consequence, the prescription in Eq. (3) is no longer a prescription to remove unwanted center-of-mass excitations, but a prescription to remove something else. Still, whatever the restricted $H_{\rm c.m.}$ is in the model space, it is the operator most closely connected with the true one. Hence, rather than removing unwanted excitations, which is now impossible in general, we may try to assess and control the damage by using Eq. (3) to construct a set of states $|\beta_{\rm c.m.}\rangle$ and see how $\langle\beta_{\rm c.m.}|H|\beta_{\rm c.m.}\rangle$ behaves. Since the problem is variational, the best we can do is choose a $\beta_{\rm c.m.}$ that minimizes the energy.

Before proceeding, it is worth going quickly through the history of the subject, under the light of these very elementary considerations which are often ignored, thereby creating unnecessary confusion. The pioneers of the subject were Elliott and Skyrme [14] who treated a simple case, the $1\hbar\omega JT^\pi=1^-0$ excitations on a sp shell core, showing that one of them was simply the $1\hbar\omega$ center-of-mass state. Other early important contributions are [18,19]. The first cross-shell calculation in a full space appeared in 1968 [20]: $(p_{1/2}s_{1/2}d_{5/2})^n$, which successfully accounted for the spectra in the region around ^{16}O. The $(p^1_{1/2}s_{1/2})J^\pi T=1^-0$ state contained a spurious component of 5.556% of the Elliott-Skyrme state. Nonetheless, Gloeckner and Lawson [21] decided to apply Eq. (3) with an arbitrarily large $\beta_{\rm c.m.}$ to eliminate the spurious components; by not realizing that $H_{\rm c.m.}$ restricted to that small space generated very little center-of-mass excitations and many genuine ones, they managed to eliminate the latter rather than the former. In spite of the criticism that ensued [22,23] showing that the procedure could not possibly make sense (except in complete spaces), no formally satisfactory arguments were advanced to replace it. Equation (3) remained a guide on where to begin to minimize the center-of-mass nuisance, and it is indeed the basis of our variational suggestion. New projection techniques have been developed [24], but they rely on explicit construction of the spurious states and they are not applicable in SMMC calculations.

The recipe advocated by Whitehead *et al.* [23] seems quite compatible with the constrained variation sketched above, and we have adopted it, since it proves sufficient to optimize the solutions. The idea is to add $\beta_{\rm c.m.}H_{\rm c.m.}$ to H, but with $\beta_{\rm c.m.}$ remaining fairly small. We have found that $\beta_{\rm c.m.}=1$ works reasonably well. This value will push spurious components up in energy by $\hbar\omega=45A^{-1/3}-25A^{-2/3}$ MeV $\simeq 14$ MeV while leaving the desired components relatively unscathed. A smaller value of $\beta_{\rm c.m.}$ leaves the spurious configurations at low enough energies that they are included in the Monte Carlo sampling, while larger values of $\beta_{\rm c.m.}$ (>3) begin to remove the entire pf shell from the calculation and artificially truncate the space. Technically, $H_{\rm c.m.}$ suffers from the sign problem, and we have to say a word about it.

SMMC methods reduce the imaginary-time, many-body evolution operator to a coherent superposition of one-body evolutions in fluctuating one-body fields. This reduction is achieved via a Hubbard-Stratonovich transformation and the resulting path integral is evaluated stochastically. SMMC methods have been applied to numerous full-basis $0\hbar\omega$ studies. The primary difficulty in these applications arises from a sign problem due to the repulsive part of effective nucleon-nucleon interactions. A practical solution to this sign problem was obtained by considering a set of Hamiltonians close to the desired realistic Hamiltonian (H) and extrapolating to the realistic case [25]. This technique has been validated in numerous studies that show the SMMC approach to be a viable and productive avenue to study extremely large many-body problems [11–13].

The original sign problem for realistic interactions was solved by breaking the two-body interaction into ''good'' (without a sign problem) and ''bad'' (with a sign problem) parts: $H=H_{\rm good}+H_{\rm bad}$. The bad part is then multiplied by a parameter g, with values typically lying in the range $-1\leqslant g\leqslant 0$. The Hamiltonian $H=f(g)H_{\rm good}+gH_{\rm bad}$ has no sign

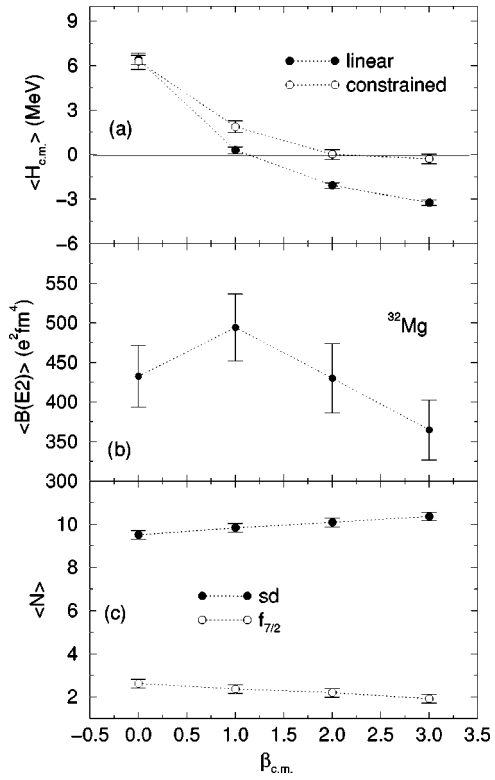

FIG. 1. (a) The calculated value of $\langle H_{\mathrm{c.m.}}\rangle$ as a function of $\beta_{\mathrm{c.m.}}$ for ^{32}Mg. Two different extrapolations were performed as described in the text. The center-of-mass contamination is already significantly reduced at $\beta_{\mathrm{c.m.}}=1$. (b) The calculated total $B(E2,0^+ \rightarrow 2^+)$ as a function of $\beta_{\mathrm{c.m.}}$. (c) The sd-shell and $f_{7/2}$-subshell occupations as a function of $\beta_{\mathrm{c.m.}}$.

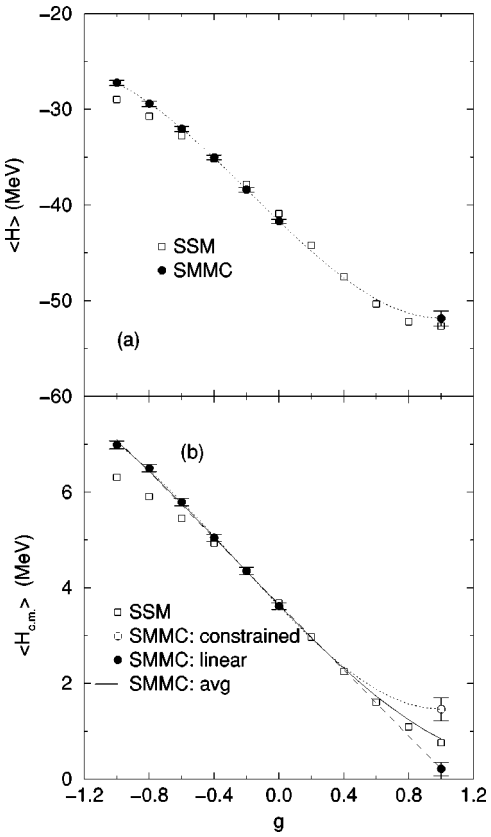

FIG. 2. (a) The expectation of the Hamiltonian, $\langle H\rangle$, for ^{22}Mg as a function of the extrapolation parameter g. Shown are standard shell-model results and SMMC results. (b) The expectation of the center-of-mass Hamiltonian, $\langle H_{\mathrm{c.m.}}\rangle$, as a function of g. SMMC results are shown for two types of extrapolation procedures, as discussed in the text, and are compared to standard shell-model results.

problem for g in this range. The function $f(g)$ is used to help in extrapolations. It is constructed such that $f(g=1)=1$, and takes the form $[1-(1-g)/\chi]$, with $\chi=4$. The SMMC observables are evaluated for a number of different negative g values and the true observables are obtained by extrapolation to $g=1$. If we fix the sign problem in the same manner as above for $H_{\mathrm{c.m.}}$, we are no longer dealing with a Hamiltonian that pushes *all* spurious components to higher energies — some components might even be lowered for $g<0$. We will see shortly that this is not a real problem.

We typically choose a minimal extrapolation (linear, quadratic, etc.) in the extrapolation parameter that gives a χ^2 per datum of $\simeq 1$. In much of our work most quantities extrapolate either linearly or quadratically. We measure the center-of-mass contamination by calculating the expectation value of $H_{\mathrm{c.m.}}$. In Fig. 1(a), we show the value of $\langle H_{\mathrm{c.m.}}\rangle$ in ^{32}Mg for several different values of $\beta_{\mathrm{c.m.}}$.[1] It is apparent that $\langle H_{\mathrm{c.m.}}\rangle$ decreases as $\beta_{\mathrm{c.m.}}$ increases. We also find that near $\beta_{\mathrm{c.m.}}=1$, $\langle H_{\mathrm{c.m.}}\rangle \ll 2\hbar\omega \simeq 28$ MeV showing that the center-of-mass contamination is minimal. Note that at approximately $\beta_{\mathrm{c.m.}}=1.5$ the average of the two different techniques of extrapolation presented in Fig. 1(a) gives $\langle H_{\mathrm{c.m.}}\rangle \simeq 0$ MeV, and the calculations could be fine-tuned for each nucleus to obtain this value.

Figure 1(a) contains two different data sets corresponding to two different methods of extrapolating $\langle H_{\mathrm{c.m.}}\rangle$ to the physical case ($g=1$). The solid circles show the results of a simple linear extrapolation where for this observable χ^2 per datum is approximately 1. It has been established [11] that $\langle H\rangle$ obeys a variational principle such that the extrapolating curve must have a minimum (slope = 0) at the physical value ($g=1$). As we sample values of the quantity $\tilde{H}$, it is perhaps reasonable to extrapolate $\langle H_{\mathrm{c.m.}}\rangle$ using this constraint as well (if $\tilde{H}$ were truly separable, this would be an exact procedure). A cubic extrapolation embodying this constraint corresponds to the open circles in Fig. 1(a).

We may further evaluate our extrapolation procedures by comparing SMMC and the standard shell-model results in ^{22}Mg. Shown in Fig. 2(a) is a detailed comparison for the expectation of the energy $\langle H\rangle$, and in Fig. 2(b) a comparison for $\langle H_{\mathrm{c.m.}}\rangle$. The standard shell-model results were obtained using the code ANTOINE [26]. The SMMC results in Fig. 2(a) employ a constrained fit such that $d\langle H\rangle/dg|_{g=1}=0$. The slight deviation from the standard shell model at $g=-0.6$, -0.8, -1.0 is due to increasing interaction matrix elements (with g), while $\Delta\beta$, the imaginary-time step, is kept fixed.

[1]All calculations presented here were performed in the zero-temperature formalism [13] using a cooling parameter of $1/\beta=0.5$ MeV with $\Delta\beta=1/32$ MeV^{-1}. These values have been shown to be sufficient to isolate the ground state for even-even nuclei. For all data presented here 4096 samples were taken at each value of the extrapolation parameter g.

This deviation is also seen in Fig. 2(b). Note that in Fig. 2(b) neither the constrained fit nor the linear fit (both with χ^2 per datum $\simeq 1$) give a precise description of the standard shell-model results at $g=1$. An average of the two ways of extrapolation, as indicated by the solid line in Fig. 2(b), apparently gives the more precise result, and we shall do this for other $H_{\text{c.m.}}$ values quoted throughout this paper. The error bar for such an averaged result is given by adding in quadrature the individual errors of both extrapolations.

In Fig. 1(b) we show the evolution of the total $B(E2)$ and in Fig. 1(c) we show the occupation of the sd shell and the $f_{7/2}$ shell as a function of $\beta_{\text{c.m.}}$. Note that the occupation of the $f_{7/2}$ orbit decreases as $\beta_{\text{c.m.}}$ increases. This is due to a combination of the removal of actual center-of-mass excitations and the ''pushing up'' in energy of the real states. The $B(E2)$ decreases slowly with $\beta_{\text{c.m.}}$, although the uncertainties are consistent with a constant. However, the decrease, particularly at $\beta_{\text{c.m.}}=3$, is likely to be real since we are working in an incomplete $n\hbar\omega$ model space. At extremely large values of $\beta_{\text{c.m.}}$ we would remove the pf shell from the calculation and return to the pure sd-shell result, which is substantially smaller than the result shown here. The slow evolution of the $B(E2)$ with $\beta_{\text{c.m.}}$ does open the intriguing possibility of studying $B(E2)$'s with an interaction that has no sign problem (e.g., pairing+quadrupole) and no center-of-mass correction with the hope of obtaining reasonable results.

Somewhere between $\beta_{\text{c.m.}}=3$ and 5, $\beta_{\text{c.m.}}H_{\text{c.m.}}$ begins to change so strongly as a function of g that our extrapolations become unreliable and we can extract no useful information. By $\beta_{\text{c.m.}}=5$, the extrapolated values become completely unreasonable, and numerical noise completely swamps the calculation. We thus conclude that a safe value for a generic study is $\beta_{\text{c.m.}}=1$, although for a given nucleus this value may be fine-tuned to nearly eliminate all center-of-mass contamination from the statistical observables. This may be done in future studies.

III. EFFECTIVE INTERACTION

Numerous shell-model studies have been carried out in truncated model spaces for neutron-rich nuclei near $N=20$ [6,8,7] and $N=28$ [2,3,9]. The number of sd-pf shell effective interactions used almost exceeds the number of papers, but there are similarities between them. A common feature is Wildenthal's universal sd shell (USD) interaction [27] to describe the pure sd-shell part of the problem. All also use some corrected version of the original Kuo-Brown (KB) G-matrix interaction [28] to describe nucleons in the pf shell. The cross-shell interaction is handled in one of two different ways: matrix elements are generated via a G matrix or via the Millener-Kurath potential. As is common in this type of calculation, selected two-body matrix elements and single-particle energies have been adjusted to obtain agreement with experiment. As these interactions have been produced for use in highly truncated spaces (usually with only $2p2h$ neutron excitations to the pf shell), they are not suitable for use in the full space. We found that they generally scatter too many particles from the sd to the pf shell, and that the $B(E2)$ values cannot be consistently calculated. We are not saying that the interactions are wrong, but that we did not succeed in adapting them to the full space. Perhaps it can be done, but it would be of limited interest; the years of experience these forces embody cannot be transposed to other spaces, as the pf-sdg shells, for instance, where detailed fits are unthinkable. Therefore, we derived a new effective interaction for the region: a monopole corrected renormalized G matrix, derived from a modern potential.

As noted in Sec. I, if G matrices have not been widely used, it is because they were thought to be so flawed as to serve at best as input parameters to overall fits, as in the case of the famous USD interaction [27]. However, it was pointed out 20 years ago [29] that practically all the problems of the KB interaction amounted to the failure to produce the $N,Z=28$ closure, and could be corrected by changing at most four centroids of the interaction. A perturbative treatment in the beginning of the pf shell using these modifications (the KB3 interaction) gave good results [30], and when the ANTOINE code became available [26], the results became truly excellent ([31,32] and references therein). In the meantime, it was confirmed in other regions that the only trouble with the G matrices resided in their centroids, i.e., in the bad saturation and shell formation properties of the realistic potentials [16]. The rest of the interaction was excellent, and strongly dominated by collective terms (pairing and quadrupole mainly) [33]. We say interaction and not interactions, because all the realistic ones produce very similar good multipole matrix elements and similar monopole failures. The outstanding problem is to replace case-by-case modifications by a general specification of H_m, the monopole field, that yields all the centroids once and for all. In Sec. III B we shall describe the proposed solution [17] we have adopted.

There is great advantage in the SMMC context to adopt the schematic collective multipole Hamiltonian (H_M) of [33], because its main terms have good signs, thereby eliminating extrapolation uncertainties; however, it may be a premature step. For one thing, it has not been established yet that in the light nuclei the collective contribution is sufficient to give high-quality results, a project better left to exact diagonalizations where fine details may be better probed. Furthermore, the renormalization treatment in [33] is somewhat crude. A more complete treatment might yield significant differences. This could be true even though potentials consistent with the NN data yield very similar collective contributions and are therefore reasonably well fitted even by older potentials. Finally, even if it were true that realistic interactions are interchangeable, and that a crude treatment of renormalization was adequate, there would certainly be no objection to using the best forces and the most sophisticated renormalizations available. In practice this is what we do here.

A. Renormalized G matrix

In order to obtain a microscopic effective shell-model interaction which spans both the $1s0d$ and the $0f1p$ shells, our many-body scheme starts with a free nucleon-nucleon interaction V which is appropriate for nuclear physics at low and intermediate energies. At present there are several potentials available. The most recent versions of Machleidt and co-workers [34], the Nimjegen group [35], and the Argonne group [36] have a χ^2 per datum close to 1 with respect to the

Nijmegen database [37]. The potential model of Ref. [34] is an extension of the one-boson-exchange models of the Bonn group [38], where mesons like π, ρ, η, δ, ω, and the fictitious σ meson are included. In the charge-dependent version of Ref. [34], the first five mesons have the same set of parameters for all partial waves, whereas the parameters of the σ meson are allowed to vary. The recent Argonne potential [36] is also a charge-dependent version of the Argonne $V14$ [39] potential. The Argonne potential models are local potentials in coordinate space and include a π exchange plus parametrizations of the short-range and intermediate-range parts of the potential. The Nimjegen group [35] has constructed potentials based on meson exchange and models parametrized in ways similar to the Argonne potentials. Another important difference between, e.g., the Bonn potentials and the Argonne and Nimjegen potentials is the strength of the much-debated tensor force [40]. Typically, the Bonn potentials have a smaller D-state admixture in the deuteron wave function than the Argonne and Nimjegen potentials, as well as other potential models. A smaller (larger) D-state admixture in the ground state of the deuteron means that the tensor force is weaker (stronger). The strength of the tensor force has important consequences in calculations of the binding energy for both finite nuclei and infinite nuclear matter (see, e.g., the discussion in Ref. [15]). A potential model with a weak tensor force tends to yield more attraction in a nuclear system than a potential with a strong tensor force; however, all these modern nucleon-nucleon interactions yield very similar excitation spectra. Moreover, in calculations of Feynman-Goldstone diagrams in perturbation theory, a potential with a weak tensor force tends to suppress certain intermediate states of long-range character, like particle-hole excitations [41]. In this paper, we choose to work with the charge-dependent version of the Bonn potential models, as found in Ref. [34].

The next step in our many-body scheme is to handle the fact that the repulsive core of the nucleon-nucleon potential V is unsuitable for perturbative approaches. This problem is overcome by introducing the reaction matrix G given by the solution of the Bethe-Goldstone equation

$$G = V + V\frac{Q}{\omega - H_0}G, \tag{4}$$

where ω is the unperturbed energy of the interacting nucleons, and H_0 is the unperturbed Hamiltonian. The projection operator Q, commonly referred to as the Pauli operator, prevents the interacting nucleons from scattering into states occupied by other nucleons. In this work, we solve the Bethe-Goldstone equation for several starting energies Ω, by way of the so-called double-partitioning scheme discussed in Ref. [15]. For the closed-shell core in the G-matrix calculation we choose ^{16}O and employ a harmonic-oscillator basis for the single-particle wave functions, with an oscillator energy $\hbar\Omega$ given by $\hbar\Omega = 45A^{-1/3} - 25A^{-2/3} = 13.9$ MeV, $A = 16$ being the mass number.

Finally, we briefly sketch how to calculate an effective two-body interaction for the chosen model space in terms of the G matrix. Since the G matrix represents just the summation to all orders of ladder diagrams with particle-particle diagrams, there are obviously other terms which need to be included in an effective interaction. Long-range effects represented by core-polarization terms are also needed. The first step then is to define the so-called $\hat{Q}$ box given by

$$P\hat{Q}P = PGP + P\left(G\frac{Q}{\omega - H_0}G + G\frac{Q}{\omega - H_0}G\frac{Q}{\omega - H_0}G + \cdots \right)P. \tag{5}$$

The $\hat{Q}$ box is made up of nonfolded diagrams which are irreducible and valence linked. We can then obtain an effective interaction $H_{\rm eff} = \tilde{H}_0 + V_{\rm eff}$ in terms of the $\hat{Q}$ box with [15]

$$V_{\rm eff}(n) = \hat{Q} + \sum_{m=1}^{\infty} \frac{1}{m!}\frac{d^m\hat{Q}}{d\omega^m}\{V_{\rm eff}^{(n-1)}\}^m, \tag{6}$$

where (n) and $(n-1)$ refer to the effective interaction after n and $n-1$ iterations. The zeroth iteration is represented by just the $\hat{Q}$ box. Observe also that the effective interaction $V_{\rm eff}(n)$ is evaluated at a given model space energy ω, as is the case for the G matrix as well. Here we choose $\omega = -20$ MeV. The final interaction is obtained after folding results in eigenvalues which depend rather weakly on the chosen starting energy (see, e.g., Ref. [42] for a discussion). All nonfolded diagrams through second order in the interaction G are included. For further details, see Ref. [15]. Finally, the reader should note that when one defines an effective interaction for several shells, the effective interaction may be strongly non-Hermitian. This non-Hermiticity should arise already at the level of the G matrix. However, since the G matrix is calculated at a fixed starting energy for both incoming and outgoing states, it is by construction Hermitian. Since we are calculating an effective interaction at a fixed starting energy, the individual diagrams entering the definition of the $\hat{Q}$ box are thereby also made Hermitian. The non-Hermiticity which stems from folded diagrams is made explicitly Hermitian through the approach of Suzuki *et al.* in Ref. [43].

B. Monopole field

As results concerning the monopole field are scattered through many papers [16,33,44,45], the most relevant of which is not yet published [17], this subsection offers a compact presentation of the main ideas.

The centroids we have often mentioned are — in a neutron proton (np) representation — the average matrix elements

$$V_{rs}^{xx'} = \frac{\sum_J (2J+1)V_{rsrs}^{Jxx'}}{\sum_J (2J+1)}, \tag{7}$$

where xx' stands for neutrons or protons in orbits rs, *respectively*. Technically, the monopole field H_m is that part of the interaction containing all the quadratic two-body forms in

scalar products of fermion operators $a^{\dagger}_{rx}\cdot a_{sx'}$ (same parity for r and s). The clean extraction of these forms from the total H (i.e., the separation $H=H_m+H_M$, M for multipole) is not altogether trivial [44]. It is conceptually important because it makes H_m closed under unitary transformations of the $a^{\dagger},a$ operators, and therefore closed under spherical Hartree-Fock variation. The expectation values we may want to vary are those of the H^d_m, the diagonal part of H_m in a given basis. Calling m_{rx} the x-number operator for orbit r, we obtain

$$H^d_m=\sum_{rx,sx'} V^{xx'}_{rs}\, m_{rx}(m_{sx'}-\delta_{rs}\delta_{xx'}), \tag{8}$$

a standard result (it is the extraction of the nondiagonal terms that is more complicated). The expectation value of H^d_m for any state is the average energy of the configuration to which it belongs (a configuration is a set of states with fixed m_{rx} for each orbit). In particular, H^d_m reproduces the exact energy of closed shells (cs) and single-particle (or hole) states built on them [(cs)$\pm$1], since for this set (cs$\pm$1) each configuration contains a single member. Consequently, it is uncontaminated by direct configuration mixing. As an example, in ^{56}Ni, the two-body (no Coulomb) contribution to the binding energy in the pf shell is approximately 73 MeV, and configuration mixing (i.e., H_M) is responsible for only 5 MeV; the rest is monopole. If we compare to the *total* binding of 484 MeV, it is clear that the monopole part becomes overwhelming, even allowing for substantial cross-shell mixing (which, incidentally, is included in the present calculations).

Therefore, H^d_m is responsible entirely for the bulk $O(A)$ and surface energies $O(A^{2/3})$, and for a very large part of the shell effects [$O(A^{1/3})$, i.e., the 73 MeV]. There can be little doubt this is where the trouble comes in the realistic potentials.

In a nutshell, the idea in [17] is to fit H^d_m to the (cs)$\pm$1 set, the single-particle and single-hole spectra around doubly magic nuclei. It is assumed that the bulk and surface terms can be separated, and by canceling the kinetic energy $K=\hbar\omega/2\Sigma_p(p+3/2)m_p$, m_p is the number of particles in harmonic oscillator (HO) shell p, against the collective monopole term [33,45], the leading term in H_m. Defining $W=\hbar\omega\Sigma_p(m_p/\sqrt{D_p})^2/4$, one obtains an expression of order $O(A^{1/3})$ that has strong shell effects producing the HO closures. To this one adds $l\cdot s$ and $l\cdot l$ one-body terms that produce the observed splittings around HO closures. The filling order is now established, and as the largest orbit – which comes lowest — is full, it alters significantly the splitting of its neighbors (e.g., the spectrum of ^{57}Ni is totally different from that of ^{41,49}Ca). This is taken care of by strictly two-body terms. With a total of six parameters (two for the $W-4K+l\cdot s+l\cdot l$ part and four for the two-body contributions), the fit yields a rms deviation of 220 keV for 90 data points.

All terms have a common scaling in $\hbar\omega=40/\rho$, obtained using a very accurate fit to the radii $\langle r^2\rangle=0.9\rho A^{1/3}$, where

$$\rho=\{A^{1/3}[1-(2T/A)^2]\}e^{(3.5/A)}. \tag{9}$$

Note that due to this scaling it is possible to use the same functional form from $A=5$ to $A=209$.

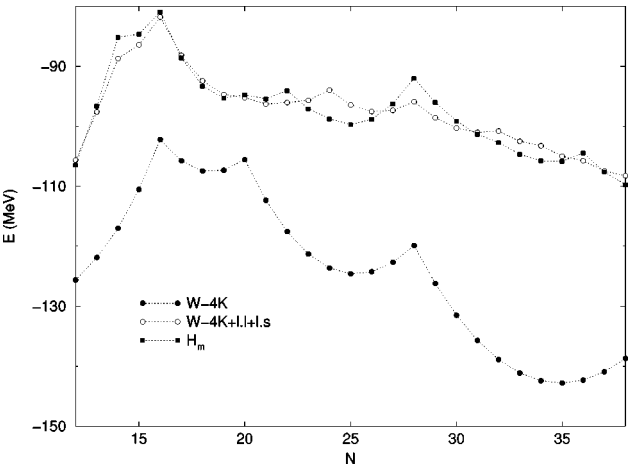

FIG. 3. Monopole shell effects in the binding energies of $T=4$ nuclei.

Figure 3 shows the mechanism of shell formation for nuclei with $T=4$. There is an overall *unbinding* drift of $O(A^{1/3})$, with pronounced HO closures due to $W-4K$ at $(N,Z)=(16,8)$, (20,12), and (28,20). The addition of the $l\cdot s+l\cdot l$ terms *practically destroys* the closures except for the first (^{24}O), and creates a fictitious one at ^{40}S. It is only through the two-body terms that closure effects reappear, but now the magic numbers are 6 (^{20}C), 14 (^{20}C,^{36}Si), and 28 (^{48}Ca,^{64}Ni). Note that the shell effect in ^{32}Mg is minuscule. The same is true for ^{30}Ne among the $T=5$ nuclei. Among the four two-body terms in H_m, there is one that is overwhelmingly responsible for the new (EI, for intruder, extruder) magic numbers. It produces an overall ($T=1$, mainly) repulsion between the largest (extruded) orbit of the shell and the others. The extruder becomes the intruder in the shell below. *This is the term that is missing in the realistic interactions*. The problems in the excitation spectra of ^{47}Ca, ^{48}Ca, and ^{49}Ca [29,15] disappear if the realistic centroids are replaced by those — even more realistic, apparently — of H_m.

To close this subsection we give some useful formulas to relate the np and isospin (mT) representations. We have

$$H^d_{mT}=K+\sum_{r\leqslant s}\frac{1}{(1+\delta_{rs})}\left[a_{rs}m_r(m_s-\delta_{rs})+b_{rs}\left(T_r\cdot T_s-\frac{3}{4}m\delta_{rs}\right)\right], \tag{10}$$

which reproduces the average energies of configurations at fixed m_rT_r.

Calling $D_r=2j_r+1$ the degeneracy of orbit r, we rewrite the relevant centroids incorporating explicitly the Pauli restrictions:

$$V_{rx,sx'}=\frac{\sum_J V^{Jxx'}_{rsrs}(2J+1)[1-(-)^J\delta_{rs}\delta_{xx'}]}{D_r(D_s-\delta_{rs}\delta_{xx'})},$$

TABLE I. Single-particle energies used in this study compared to the two sets in Refs. [17].

jp	SPE old	SPE new	SPE calc.
$d_{5/2}$ 3	16.679	15.193	15.129
$s_{1/2}$ 3	12.454	12.719	12.629
$d_{3/2}$ 3	10.404	10.543	10.629
$f_{7/2}$ 3	9.022	8.324	8.629
$p_{3/2}$ 2	6.381	6.133	5.595
$p_{1/2}$ 2	1.336	0.722	0.784
$f_{5/2}$ 2	0.000	0.000	0.000

$$V_{rs}^{T}=\frac{\sum_{J} V_{rsrs}^{JT}(2J+1)[1-(-)^{J+T}\delta_{rs}]}{D_r[D_s+\delta_{rs}(-)^{T}]}, \tag{11}$$

$$a_{rs}=\frac{1}{4}(3V_{rs}^{1}+V_{rs}^{0}), \quad b_{rs}=V_{rs}^{1}-V_{rs}^{0}. \tag{12}$$

In the np scheme each orbit r goes into two rx and rx' and the centroids can be obtained through $x\neq x'$:

$$V_{rx,sx'}=\frac{1}{2}\left[V_{rs}^{1}\left(1-\frac{\delta_{rs}}{D_r}\right)+V_{rs}^{0}\left(1+\frac{\delta_{rs}}{D_r}\right)\right],$$

$$V_{rx,sx}=V_{rs}^{1}. \tag{13}$$

C. Monopole terms in the calculations

The calculations used the preliminary version of H_m [17], which for the purposes of this study should make little difference. All we have said above is valid for both the old and the new version except for details. Only one of them is worth mentioning here, and it concerns the single-particle energies shown in Table I. It is seen that the old and new values are quite close to those adopted in the calculations, though the old set puts the $s_{1/2}$ and $f_{5/2}$ orbits higher. This reflects the awkward behavior of the $l\cdot l$ part of H_m that changes sign at the $p=3$ shell. This problem was treated artificially in the old version through a single-particle mechanism that was discarded in the calculations, mainly because keeping it would have demanded a readjustment of the interaction for each nucleus — an unwanted complication in a feasibility study such as this one. As a consequence, we expect the $s_{1/2}$ orbit to be overbound with respect to its sd partners in the upper part of the shell. In the new version the mechanism becomes two-body and should do much better.

There has been much discussion about the choice of the cross-shell gap, i.e., the distance between the $d_{3/2}$ and $f_{7/2}$ orbits, which plays a crucial role in all truncated calculations. It could be thought from Table I that it is rather small. But this is an illusion since H_m will make it evolve. In ^{29}Si it will increase to 4.5 MeV ($\approx$500 keV above experiment), which grows up to 5.2 MeV in ^{40}Ca, now too small with respect to the binding energy (BE) difference $2\mathrm{BE}(^{40}\mathrm{Ca})-\mathrm{BE}(^{41}\mathrm{Ca})-\mathrm{BE}(^{39}\mathrm{Ca})=7.2$ MeV. The only way to decide whether these positionings are correct is through calculations such as the present ones. We return to this issue in Sec. IV.

The analysis of binding energies is a delicate exercise because external parameters have to be introduced. The philosophy behind H_m is to make all calculations *coreless*. Because of the $\hbar\omega$ propagation (which should be extended to H_M), nuclei readjust their sizes and energies as N and Z change. If the bulk terms are added, there is, in principle, no need to fit anything, and the calculated energies are absolute — not referred to any core. In the present calculations the interaction was kept fixed, and the way to proceed is the traditional one, by referring all energies to the core of ^{16}O. First, we estimate Coulomb effects using $V_c=0.717Z(Z-1)(A^{-1/3}-A^{-1})$, and then fit

$$H_{\mathrm{corr}}=\varepsilon m+a\frac{m(m-1)}{2}+b\frac{T(T+1)-3m/4}{2}. \tag{14}$$

It is generally assumed that ε should be close to the single-particle energy of ^{17}O(-4.14 MeV) and that the quadratic terms are the average H_{mT} over the space [from Eq. (10)]. However, these assumptions do not apply here. The contribution to b from H_{mT} is relatively small. The symmetry energy must be counted as one of the bulk terms, and the best we can do is to take it from fits to the binding energies, which yield consistently similar numbers. From [45] we adopt the form $\mathcal{S}=22[4T(T+1)](1-1.82/A^{1/3})/A$, where the main term has been reduced by the approximately 6 MeV coming from H_m. We cannot change these parameters; we can only check that the fit to H_{corr} yields a b consistent with them. But there is subtlety: the isospin term vanishes at $m=1$ because it is taken to be two-body, while $\mathcal{S}$ gives a substantial 1.15 MeV contribution at ^{17}O. Therefore, to use the form of H_{corr}, ε must be $\mathcal{S}$ corrected (in the same sense that we Coulomb correct) to $-4.14-1.15=-5.29$ MeV. For b we must take some average $\mathcal{S}$, which we choose to be the value at $A=40$, i.e., $b=2.34$. Finally for a we must expect a small value, since it should come entirely from H_m. The fit yields (in MeV) $\varepsilon=-5.34$, $a=-0.319$, and $b=1.99$ and a χ^2 per degree of freedom of 3.12. While ε and b are very comfortably close to our expectations, a is much too large. But that is not a problem: the program that transforms H_m into V_{rs}^{T} had been thoroughly checked for excitation energies but not for binding energies. It had a bug in it that accounts for nearly -250 keV in the a term. Hence, when $\mathcal{S}$ is taken into account and the bug is corrected, the fit becomes (in keV) $\varepsilon=-50$, $a=-59$, and $b=235$. The numbers are now pleasingly small and the principal uncertainty stems from the parameters in $\mathcal{S}$.

Our mass results are shown in Figs. 4(a) and 4(b). While there is both underbinding and overbinding of the nuclei studied, the agreement is reasonably acceptable. It becomes remarkable if we consider that — in view of the smallness of H_{corr} — it is practically parameter free. For completeness, in Fig. 4(c) we show $\langle H_{\mathrm{c.m.}}\rangle$ for the same nuclei. Notice that for the nuclei above mass 40 the center-of-mass contamination could be further corrected by fine-tuning $\beta_{\mathrm{c.m.}}$. However, for our present purposes, we will be content with the removal of much of the center-of-mass energy.

As a final example of the soundness of the interaction, we show in Fig. 5 a number of low-lying states for ^{22}Mg calculated by direct diagonalization in the full sd-pf space, compared to both a sd-shell calculation using the USD interac-

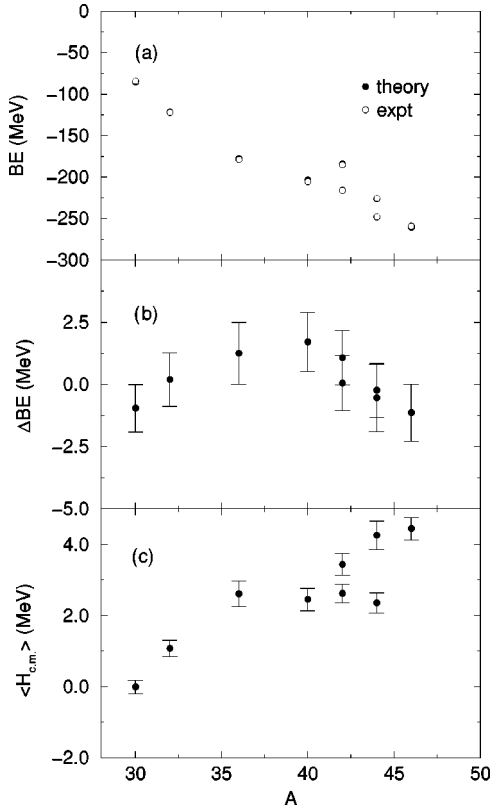

FIG. 4. (a) The binding energy relative to the ^{16}O core for various nuclei in this study. (b) The difference between experiment and theory for these nuclei. (c) The expectation of the center-of-mass Hamiltonian for the nuclei calculated in this study.

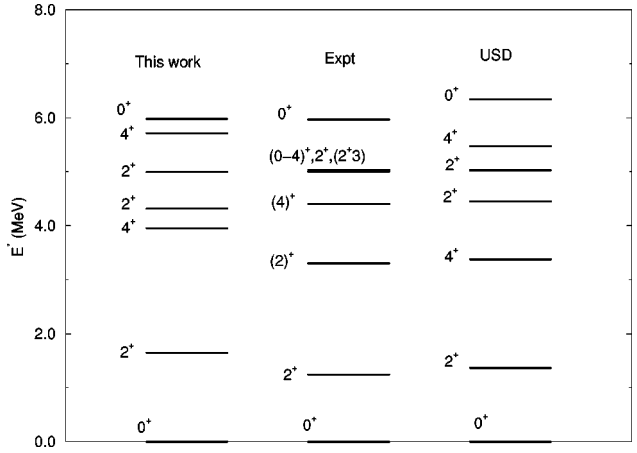

FIG. 5. Theoretical and experimental level spectra for ^{22}Mg are compared. The left spectrum is obtained from the Hamiltonian described in the text. USD is the Wildenthal sd-shell interaction used in a sd-shell calculation for comparison.

tion and to experiment [46]. Generally, our interaction agrees reasonably well with both experiment and the USD interaction. The more refined treatment of H_m will no doubt further improve the agreement. We also note that we have checked the center-of-mass contamination for all of the excited states shown in the first column of Fig. 5, and it is as small as that shown for the ground state in Fig. 2.

IV. RESULTS

A. Comparison with experiment and other calculations

There is limited experimental information about the highly unstable, neutron-rich nuclei under consideration. In many cases only the mass, excitation energy of the first excited state, the $B(E2)$ to that state, and the β-decay rate are known, and not even all of this information is available in some cases. From the measured $B(E2)$, an estimate of the nuclear deformation parameter β_2 has been obtained via the usual relation

$$\beta_2 = 4\pi\sqrt{B(E2;0^+_{\text{g.s.}}\rightarrow 2^+_1)}/3ZR_0^2e, \tag{15}$$

with $R_0 = 1.2A^{1/3}$ fm and $B(E2)$ given in e^2 fm^4.

Much of the interest in the region stems from the unexpectedly large values of the deduced β_2, results which suggest the onset of deformation and have led to speculations about the vanishing of the $N=20$ and $N=28$ shell gaps. The lowering in energy of the 2^+_1 state supports this interpretation. The most thoroughly studied case, and the one which most convincingly demonstrates these phenomena, is ^{32}Mg with its extremely large $B(E2) = 454 \pm 78\, e^2$ fm^4 and corresponding $\beta_2 = 0.513$ [1]; however, a word of caution is necessary when deciding on the basis of this limited information that we are in the presence of well-deformed rotors: for ^{22}Mg, we would obtain $\beta_2 = 0.67$, even more spectacular, and for ^{12}C, $\beta_2 = 0.8$, well above the superdeformed bands.

TABLE II. The computed and measured values of $B(E2)$ for the nuclei in this study using $e_p = 1.5$ and $e_n = 0.5$.

	$B(E2;0^+_{\text{g.s.}}\rightarrow 2^+_1)_{\text{expt}}$	$B(E2,\text{total})_{\text{SMMC}}$	$B(E2;0^+_{\text{g.s.}}\rightarrow 2^+_1)$	$B(E2,0^+_{\text{g.s.}}\rightarrow 2^+_1)_{\text{USD}}$
^{22}Mg	458±183	334±27		314.5
^{30}Ne		303±32	342 [8],171 [53]	143.2
^{32}Mg	454±78 [1]	494±44	448 [8],205 [53]	177.1
^{36}Ar	296.56±28.3 [46]	174±48		272.8
^{40}S	334±36 [2]	270±66	398 [3],390 [9]	
^{42}S	397±63 [2]	194±64	372 [3],465 [9]	
^{42}Si		445±62	260 [9]	
^{44}S	314±88 [3]	274±68	271 [3],390 [9]	
^{44}Ti	610±150 [52]	692±63		
^{46}Ar	196±39 [2]	369±77	460 [2],455 [9]	

TABLE III. The effective charges e_p and e_n used in the various truncated shell-model calculations for the nuclei in this study.

Reference	e_p	e_n
[2]	1.6	0.9
[3]	1.35	0.65
[7,9]	1.5	0.5
[8]	1.3	0.5

Most of the measured observables can be calculated within the SMMC framework. It is well known that in *deformed* nuclei the total $B(E2)$ strength is almost saturated by the $0^+_{\text{g.s.}} \rightarrow 2^+_1$ transition (typically 80%–90% of the strength lies in this transition). Thus the total strength calculated by SMMC simulations should only slightly overestimate the strength of the measured transition. In Table II the SMMC computed values of $B(E2,\text{total})$ are compared both to the experimental $B(E2;0^+_{\text{g.s.}} \rightarrow 2^+_1)$ values and to the values found in various truncated shell-model calculations. Reasonable agreement with experimental data across the space is obtained when one chooses effective charges of $e_p = 1.5$ and $e_n = 0.5$. We also indicate in the right column of Table II the USD values for the $B(E2,0^+_{\text{g.s.}} \rightarrow 2^+_1)$ (with effective charges of $e_p = 1.5$ and $e_n = 0.5$) for the sd-shell nuclei. Note that the sd-shell results are much lower for ^{30}Ne and ^{32}Mg than is seen experimentally. All of the theoretical calculations require excitations to the pf shell before reasonable values can be obtained. We note a general agreement among all calculations of the $B(E2)$ for ^{46}Ar, although they are typically larger than experimental data would suggest. We also note a somewhat lower value of the $B(E2)$ in this calculation as compared to experiment and other theoretical calculations in the case of ^{42}S. Shown in Table III are effective charges from other calculations.

Table IV gives selected occupation numbers for the nuclei considered. We first note a difficulty in extrapolating some of the occupations where the number of particles is nearly zero. This leads to a systematic error bar that we estimate at ± 0.2 for all occupations shown, while the statistical error bar is quoted in the table. The extrapolations for occupation numbers were principally linear. Table IV shows that ^{22}Mg remains as an almost pure sd-shell nucleus, as expected. We also see that the protons in ^{30}Ne, ^{32}Mg , and ^{42}Si are almost entirely confined to the sd shell. This latter is a pleasing result in at least two regards. First, it shows that the interaction does not mix the two shells to an unrealistically large extent. Second, if spurious center-of-mass contamination were a severe problem, we would expect to see a larger proton $f_{7/2}$ population for these nuclei due to the $0d_{5/2}$-$0f_{7/2}$ ''transition'' mediated by the center-of-mass creation operator. The fact that there is little proton $f_{7/2}$ occupation for these nuclei confirms that the center-of-mass contamination is under reasonable control.

An interesting feature of Table IV lies in the neutron occupations of the $N=20$ nuclei (^{30}Ne and ^{32}Mg) and the $N=28$ nuclei (^{42}Si, ^{44}S, and ^{46}Ar). The neutron occupations of the two $N=20$ nuclei are quite similar, confirming the finding of Fukunishi *et al.* [8] and Poves and Retamosa [7] that the $N=20$ shell gap is modified. In fact, the neutron $f_{7/2}$ orbital contains approximately two particles before the $N=20$ closure, thus behaving like an intruder single-particle state. Furthermore, we see that two-particle–two-hole (2p-2h) excitations dominate, although higher excitations also play some role. We also see that the neutrons occupying the pf shell in $N=20$ systems are principally confined to the $f_{7/2}$ subshell.

The conclusions that follow from looking at nuclei with $N>20$, particularly those with $N=28$, are that the $N=20$ shell is nearly completely closed at this point, and that the $N=28$ closure shell is reasonably robust, although approximately one neutron occupies the upper part of the pf shell. Coupling of the protons with the low-lying neutron excitations probably accounts for the relatively large $B(E2)$, without the need of invoking rotational behavior.

In Table V we show the SMMC total Gamow-Teller (GT^-) strength. We compare our results to those of previous truncated calculations, where available. In all cases, our results are slightly smaller than, but in good accordance with, other calculations. Since we do not calculate the strength function, we do not compute β-decay lifetimes.

B. Pairing properties

For a given angular momentum J, isospin T, and parity π, we define the pair operators as

$$A^\dagger_{JM,TT_z\pi}(ab) = \frac{(-1)^{l_a}}{\sqrt{1+\delta_{ab}}}[a^\dagger_{j_a} \times a^\dagger_{j_b}]^{JM,TT_z}, \qquad (16)$$

TABLE IV. The calculated SMMC neutron (n) and proton (p) occupation numbers for the sd shell, the $0f_{7/2}$ subshell, and the remaining orbitals of the pf shell. The statistical errors are given for linear extrapolations. A systematic error of ± 0.2 should also be included.

	N,Z	n-sd	n-$f_{7/2}$	n-$pf_{5/2}$	p-sd	p-$f_{7/2}$	p-$pf_{5/2}$
^{22}Mg	10,12	3.93±0.02	0.1±0.02	−0.05±0.01	2.04±0.02	0.00±0.01	−0.05±0.01
^{30}Ne	20,10	9.95±0.03	2.32±0.03	−0.26±0.02	2.03±0.02	−0.01±0.01	−0.02±0.01
^{32}Mg	20,12	9.84±0.03	2.37±0.03	−0.21±0.02	3.99±0.03	0.05±0.02	−0.05±0.01
^{36}Ar	18,18	9.07±0.03	1.08±0.02	−0.15±0.02	9.07±0.03	1.08±0.02	−0.15±0.02
^{40}S	24,16	11.00±0.03	5.00±0.03	−0.01±0.02	7.57±0.04	0.54±0.02	−0.12±0.02
^{42}Si	28,14	11.77±0.02	7.34±0.02	0.90±0.03	5.79±0.03	0.25±0.02	−0.07±0.01
^{42}S	26,16	11.41±0.02	6.33±0.02	0.25±0.03	7.49±0.03	0.58±0.02	−0.09±0.02
^{44}S	28,16	11.74±0.02	7.18±0.02	1.06±0.03	7.54±0.03	0.56±0.02	−0.12±0.02
^{44}Ti	22,22	10.42±0.03	3.58±0.02	0.00±0.02	10.42±0.03	3.58±0.02	0.00±0.02
^{46}Ar	28,18	11.64±0.02	7.13±0.02	1.23±0.03	8.74±0.03	1.34±0.02	−0.08±0.02

TABLE V. The calculated total Gamow-Teller strength (GT^-) from this study. The results of other studies, when available, are presented for comparison.

Nucleus	SMMC	Other
^{22}Mg	0.578±0.06	
^{30}Ne	29.41±0.25	
^{32}Mg	24.00±0.34	
^{36}Ar	2.13±0.61	
^{40}S	22.19±0.44	22.87 [9]
^{42}S	28.13±0.42	28.89 [9]
^{42}Si	40.61±0.34	
^{44}S	34.59±0.39	34.93 [9]
^{44}Ti	4.64±0.66	
^{46}Ar	29.07±0.44	28.84 [9]

where the parity is given by $(-1)^{l_a+l_b}$. These operators are boson like in the sense that they satisfy the expected commutation relations in the limit where the number of valence nucleons is small compared with the total number of single-particle states in the shell. In the SMMC calculation we compute the pair matrix in the ground state as

$$M_{JTT_z\pi}(ab,cd)=\sum_M \langle A^\dagger_{JM,TT_z\pi}(ab)A_{JM,TT_z\pi}(cd)\rangle, \tag{17}$$

which is a Hermitian and positive-definite matrix in the space of ordered orbital pairs (ab) (with $a\leqslant b$). The total number of pairs is given by

$$P_{JTT_z\pi}=\sum_{abcd} M_{JTT_z\pi}(ab,cd). \tag{18}$$

The pair matrix can be diagonalized to find the eigenbosons $B^\dagger_{\alpha JTT_z\pi}$ as

$$B^\dagger_{\alpha JMTT_z\pi}=\sum_{ab} \psi_{\alpha JT\pi}(ab)A^\dagger_{JMTT_z\pi}(ab), \tag{19}$$

where $\alpha=1,2,\ldots$ labels the various bosons with the same angular momentum, isospin, and parity. The $\psi_{\alpha JT\pi}$ are the eigenvectors of the diagonalization, i.e., the wave functions of the boson, and satisfy the relation

$$\sum_{j_aj_b} \psi^*_{\alpha JTT_z\pi}\psi_{\mu JTT_z\pi}=\delta_{\alpha\mu}. \tag{20}$$

These eigenbosons satisfy

$$\sum_M \langle B^\dagger_{\alpha JM,TT_z\pi}B_{\gamma JM,TT_z\pi}\rangle=n_{\alpha JTT_z\pi}\delta_{\alpha\gamma}, \tag{21}$$

where the positive eigenvalues $n_{\alpha JTT_z\pi}$ are the number of $JTT_z\pi$ pairs of type α.

We first show the number of pairs $P_{JTT_z\pi}$ in the $J=0$, $T=1$ positive-parity pairing channels. This quantity can be interpreted as the total strength for the pair transfer of particles of the given quantum numbers. Shown in Fig. 6 are

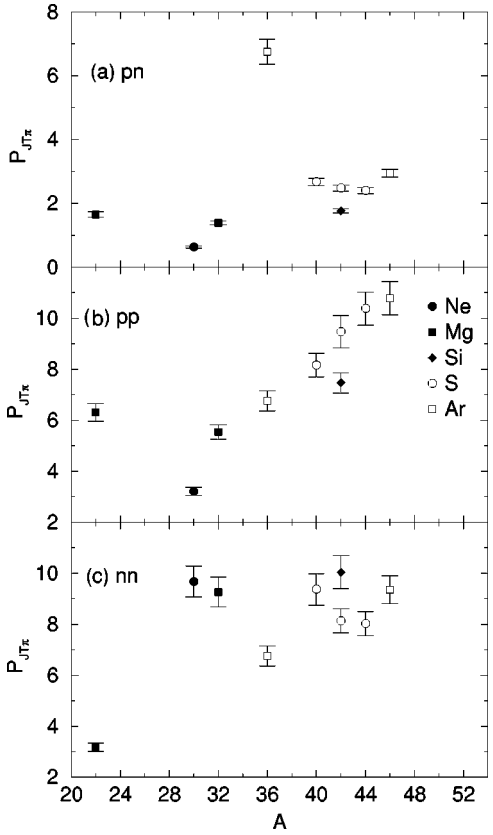

FIG. 6. The number of pairs present in the SMMC calculations for the $J^\pi T=0^+1$: (a) the $T_z=0(pn)$ channel, (b) the $T_z=1(pp)$ channel, and (c) the $T_z=-1(nn)$ channel.

our results in the proton-neutron (top), proton-proton (middle), and neutron-neutron (bottom) channels as a function of the nucleus A. Notice that only in the $N=Z$ nucleus ^{36}Ar do the proton-neutron pairs play a significant role, as has been discussed in [47]. Generally, one also sees an increase in the proton-proton pairs as A is increased. Notice also that a fair amount of increase occurs in the sulfur and argonne isotope chains as one adds neutrons. This is not the case in the two Mg isotopes calculated, in which we see a significant increase in the neutron-neutron correlations, but very little change in the proton-proton sector. This holds for both the Ne and Mg chains [48]. For the heavier isotopes in the region, in general, the $J=0$ neutron-neutron pairs are not significantly enhanced for the nuclei that we have calculated here. Since there are many more particles and hence more pairing, one expects enhancements to occur in higher J pairs since the total number of pairs is a conserved quantity for a given number of like nucleons. We also calculated the pairing in the same channels, but with negative parity ($\pi=(-1)^{l_a+l_b}=(-1)^{l_c+l_d}$), and find it to be rather small in most cases.

Further insight into the pairing comes by considering diagonal elements of the pair matrix before and after diagonalization. The presence of a pair condensate in a correlated ground state will be signaled by the largest eigenvalue for a given J being much greater than any of the others. Shown in Fig. 7 are the diagonal matrix elements of the $J=0$ pair matrix for ^{40,44}S before (left panel) and after (right panel) diagonalization. We see from the left panel that adding four

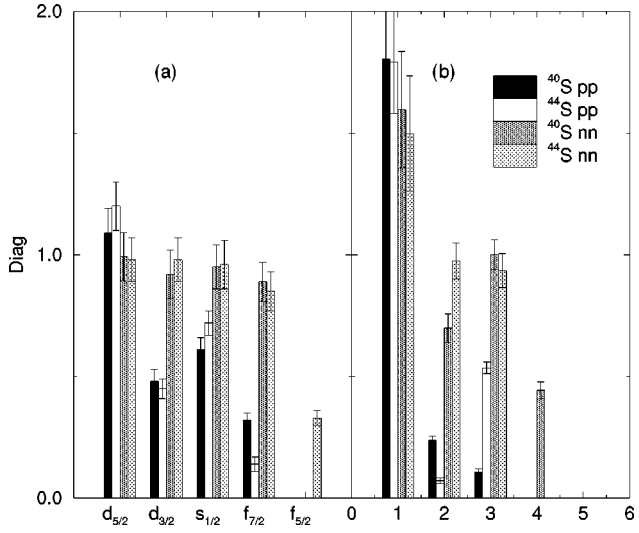

FIG. 7. Left panel: the diagonal elements of the $J=0pp$ and nn pair matrix before diagonalization. Note that proton pairing does not play a significant role in the pf shell. Right panel: the eigenvalues of the pair matrix shown in decreasing size. After diagonalization the protons have only three nonzero eigenvalues.

neutrons to the system increases the $f_{5/2}$-shell neutron matrix elements, while rearranging the sd-shell elements slightly. From the occupation numbers we know that the neutrons are filling pf-shell orbitals, and therefore we expect little movement in the sd shell. The proton matrix elements are slightly affected by the addition of the neutrons, although there is some movement of protons out of the $f_{7/2}$.

The largest eigenvalue of the neutron-neutron pair matrix, as shown in the right panel in Fig. 7, is about 1.5 times that of the next largest eigenvalue. However, the remaining eigenvalues are significant. Thus it is unlikely that there exists a pure pair condensate in the neutrons. As a further check on this conclusion, we have diagonalized the 3×3 pairing matrix resulting from only the sd-shell neutrons in these two nuclei. We find that the three eigenvalues are all of similar size and significantly smaller than the largest eigenvalue from the full sd-pf diagonalization. Thus, what neutron pair condensate does exist is a phenomenon which involves the entire model space, not just the sd shell. In the proton sector we see a similar level of pair condensation. Since the protons occupy mainly the sd shell, only three eigenvalues are large enough to be represented in the figure.

C. Discussion

The aim of a nuclear structure calculation is to compare with, or predict, experimental results. In the present case, the comparison with other calculations is at least of equal interest. The reason comes from the problems created by truncations, in particular the $(0+2)\hbar\omega$ ''catastrophe'' [6], discovered long ago in a $0\hbar\omega$ context [29]. Calling f the $f_{7/2}$ shell and r its pf partners generically, an f^n calculation can produce very sensible results; $f^n+f^{n-1}r$ improves them considerably, but $f^n+f^{n-1}r+f^{n-2}r^2$ is invariably disastrous, because the f^n configuration is strongly pushed down by pairing with $f^{n-2}r^2$, while $f^{n-1}r$ does not benefit from a similar push from $f^{n-3}r^2$. The remarkable thing is that when this last configuration is included, the results are not too different from the original $f^n+f^{n-1}r$. If the space is expanded, there is an attenuated $4\hbar\omega$ catastrophe. The process continues in increasingly attenuated form until the exact $(fr)^n$ space is reached. This is a general problem with truncations, and for nuclei such as ^{32}Mg with a $(pf)^2(sd)^{n-2}$ ground state, where the calculations demand also the presence of $(sd)^n$ states, the adopted solution has been simply to ignore the mixing between the two configurations. It works very well. But is it true? Could it not be possible that higher excitations play an important role? Fortunately, we can say that the present calculations confirm the basic validity of previous work. In all the cases we analyzed, the ''dressing'' process, whereby a dominant configuration becomes the exact ground state, does not seem to affect strongly its basic properties. Does it mean that exact calculations are unnecessary? Not exactly. For one thing, they have no parameters other than those of H_m and therefore demonstrate the validity of the monopole corrected G matrices. And then they go — for the first time in a shell-model context — to the heart of the problem of cross-shell correlations. At present, we know little about these problems, except that they are hidden so well that they are difficult to detect. Still, they can be seen through effects (such as quenching of Gamow-Teller strength) that tell us that they are important. The available evidence points to a much reduced discontinuity at the Fermi level with respect to the naive shell model [49–51]. In Table IV we find nearly normal occupancies for high T, but strong effects for $T=0$ ground states, in particular for ^{44}Ti — a truly interesting case. A conventional $(pf)^4$ calculation yields a $B(E2)$ of $514.7e^2\mathrm{fm}^4$ (virtually identical to that of KB3). In Table II the result is at least 20% larger. This is a good example of the way correlations may be hidden. No doubt this nucleus is a *bona fide* member of the pf space, and the correlation effects can be overcome by the experimental error, but it is not always the case. The region is plagued with $B(E2)$ transitions which are systematically too large for the $0\hbar\omega$ calculations to explain, particularly for the Ca isotopes, which should be the simplest nuclei, but are the most complicated. In ^{44}Ti we have a first example of what a complete calculation could do.

Binding energies are no doubt one of the best ways to shed light on the matter. In Sec. III C we mentioned the cross-shell gap around ^{40}Ca, which should be increased by about 2 MeV, which means that the correlation energy should be much larger. And since we know now that we can trust SMMC calculations with a good interaction to within 1 MeV, probably it will not take long before we know more about this supposedly closed nucleus that is not so closed.

V. CONCLUSION

This paper was meant as a feasibility study of SMMC calculations in multi-$\hbar\omega$ spaces. Two general issues had to be tackled: translational invariance and the definition of an interaction. Concerning the first, it was shown that the trouble caused by center-of-mass excitations can be successfully mitigated by a judicious application of ideas in [23], and a possible variational approach to the problem was suggested. The interaction chosen was a G matrix derived from a modern potential, renormalized according to state-of-the-

art techniques, and monopole corrected for the bad saturation properties of the existing NN potentials. The only parameters entering the calculations are the six ''universal'' constants specifying the monopole Hamiltonian, which was shown to explain quite naturally the shell formation properties of high isospin nuclei in the $A=30-50$ region.

The feasibility test was passed satisfactorily. Binding energies, $B(E2)$ rates, and Gamow-Teller strengths were obtained that are in reasonable agreement with observations, and the possible origin of the remaining discrepancies has been identified.

The calculations support the validity of previous work in the region, and open the way to the study of the elusive deep correlations at the origin of Gamow-Teller quenching. In particular it provides an example, in ^{44}Ti, of an extremely correlated system whose behavior is quite similar to that of the uncorrelated one. The possibility to obtain orbit occupancies should help in advancing the study of the discontinuity at the Fermi surface — one of the most difficult problems in nuclear physics.

Interest was focused on neutron-rich nuclei around $N=20,28$ (a region of current interest), where new data have become available and many calculations have been performed. Having established the reliability of our methods, other exotic, or not so exotic, studies can be contemplated.

Most calculations presented here were performed on the 512-node Paragon at the Oak Ridge Center for Computational Science (CCS) and the T3E at the National Energy Research Scientific Computing Center (NERSC). The sd-pf model space effectively used all of the available memory on the Paragon (32 Mbytes per node) and, hence, larger spaces were not feasible there. With the advent of a new generation of massively parallel computers that are much faster and have far more memory, much more ambitious calculations are possible.

ACKNOWLEDGMENTS

We acknowledge useful discussions with Petr Vogel and Dao-Chen Zheng. M.T.R. gratefully acknowledges support from the Weingart Foundation; he and S.E.K. were supported in part by the U.S. National Science Foundation under Grants Nos. PHY94-12818 and PHY94-20470. Oak Ridge National Laboratory is managed by Lockheed Martin Energy Research Corp. for the U.S. Department of Energy under Contract No. DE-AC05-96OR22464. K.L. acknowledges support from the Danish Research Council. Grants of computational resources were provided by the Center for Advanced Computational Research at Caltech and the Center of Computational Science at ORNL, as well as the National Energy Research Scientific Computing Center. Part of this work was conducted at the Aspen Center for Physics. D.J.D., K.L., and A.Z. acknowledge support from NATO Grant No. CRG.CRPG 973035.

[1] T. Motobayashi *et al.*, Phys. Lett. B **346**, 9 (1995).
[2] H. Scheit *et al.*, Phys. Rev. Lett. **77**, 3967 (1996).
[3] T. Glasmacher *et al.*, Phys. Lett. B **395**, 163 (1997).
[4] T. R. Werner *et al.*, Nucl. Phys. **A597**, 327 (1996).
[5] X. Campi, H. Flocard, A. K. Kerman, and S. E. Koonin, Nucl. Phys. **A251**, 193 (1975).
[6] E. K. Warburton, J. A. Becker, and B. A. Brown, Phys. Rev. C **41**, 1147 (1990).
[7] A. Poves and J. Retamosa, Nucl. Phys. **A571**, 221 (1994).
[8] N. Fukunishi, T. Otsuka, and T. Sebe, Phys. Lett. B **296**, 279 (1992).
[9] J. Retamosa, E. Caurier, F. Nowacki, and A. Poves, Phys. Rev. C **55**, 1266 (1997).
[10] E. Caurier, F. Nowacki, A. Poves, and J. Retamosa, Phys. Rev. C **58**, 2033 (1998).
[11] S. E. Koonin, D. J. Dean, and K. Langanke, Phys. Rep. **278**, 2 (1997).
[12] S. E. Koonin, D. J. Dean, and K. Langanke, Annu. Rev. Nucl. Part. Sci. **47**, 463 (1997).
[13] G. H. Lang, C. W. Johnson, S. E. Koonin, and W. E. Ormand, Phys. Rev. C **48**, 1518 (1993).
[14] J. P. Elliott and T. H. R. Skyrme, Proc. R. Soc. London, Ser. A **232**, 561 (1955).
[15] M. Hjorth-Jensen, T. T. S. Kuo, and E. Osnes, Phys. Rep. **261**, 125 (1995).
[16] A. Abzouzi, E. Caurier, and A. P. Zuker, Phys. Rev. Lett. **66**, 1134 (1991).
[17] J. Duflo and A. P. Zuker, Phys. Rev. Lett. (submitted). An earlier version can be retrieved from http://csnwww.in2p3.fr/amdc/ (theory file du_zu_ph.ps)
[18] S. Gartenhaus and C. Schwartz, Phys. Rev. **108**, 482 (1957).
[19] E. Baranger and C. W. Lee, Nucl. Phys. **22**, 157 (1961).
[20] A. P. Zuker, B. Buck, and J. B. McGrory, Phys. Rev. Lett. **21**, 39 (1968).
[21] D. H. Gloeckner and R. D. Lawson, Phys. Lett. **53B**, 313 (1974).
[22] J. B. McGrory and B. H. Wildenthal, Phys. Lett. **60B**, 5 (1975).
[23] R. R. Whitehead, A. Watt, B. J. Cole, and I. Morrison, in *Advances in Nuclear Physics*, edited by M. Baranger and E. Vogt (Plenum, New York, 1977), Vol. 9.
[24] P. K. Rath, A. Faessler, H. Müther, and A. Watts, J. Phys. G **16**, 245 (1990).
[25] Y. Alhassid, D. J. Dean, S. E. Koonin, G. Lang, and W. E. Ormand, Phys. Rev. Lett. **72**, 613 (1994).
[26] E. Caurier, computer code ANTOINE, Strasbourg, 1989.
[27] B. H. Wildenthal, in *Progress in Particle and Nuclear Physics 11*, edited by D. H. Wilkinson (Pergamon Press, Oxford, 1984), p. 5.
[28] T. T. S. Kuo and G. E. Brown, Nucl. Phys. **A85**, 40 (1966); **A114**, 241 (1968).
[29] E. Pasquini, Ph.D. thesis, Report No. CRN/PT 76-14, Strasbourg, 1976; E. Pasquini and A. P. Zuker, in *Physics of Medium Light Nuclei*, Florence, 1977, edited by P. Blasi and R. Ricci (Editrice Compositrice, Bologna, 1978).
[30] A. Poves and A. P. Zuker, Phys. Rep. **70**, 235 (1981).
[31] G. Martínez-Pinedo, A. P. Zuker, A. Poves, and E. Caurier, Phys. Rev. C **55**, 187 (1997).

[32] A. P. Zuker, in *Contemporary Shell Model*, edited by X. W. Pan (Springer, New York, 1997), p. 482.
[33] M. Dufour and A. P. Zuker, Phys. Rev. C **54**, 1641 (1996).
[34] R. Machleidt, F. Sammarruca, and Y. Song, Phys. Rev. C **53**, R1483 (1996).
[35] V. G. J. Stoks, R. A. M. Klomp, C. P. F. Terheggen, and J. J. de Swart, Phys. Rev. C **48**, 792 (1993).
[36] R. B. Wiringa, V. G. J. Stoks, and R. Schiavilla, Phys. Rev. C **51**, 38 (1995).
[37] V. G. J. Stoks, R. A. M. Klomp, C. P. F. Terheggen, and J. J. de Swart, Phys. Rev. C **49**, 2950 (1994).
[38] R. Machleidt, Adv. Nucl. Phys. **19**, 189 (1989).
[39] R. B. Wiringa, R. A. Smith, and T. L. Ainsworth, Phys. Rev. C **29**, 1207 (1984).
[40] G. E. Brown and R. Machleidt, Phys. Rev. C **50**, 1731 (1994).
[41] H. M. Sommerman, H. Müther, K. C. Tam, and T. T. S. Kuo, Phys. Rev. C **23**, 1765 (1981).
[42] P. J. Ellis, T. Engeland, M. Hjorth-Jensen, A. Holt, and E. Osnes, Nucl. Phys. **A573**, 216 (1994).
[43] K. Suzuki, R. Okamoto, P. J. Ellis, and T. T. S. Kuo, Nucl. Phys. **A567**, 565 (1994).
[44] A. P. Zuker, Nucl. Phys. **A576**, 65 (1994).
[45] J. Duflo and A. P. Zuker, Phys. Rev. C **52**, R23 (1995).
[46] P. M. Endt, Nucl. Phys. **A521**, 1 (1990).
[47] K. Langanke, D. J. Dean, S. E. Koonin, and P. B. Radha, Nucl. Phys. **A613**, 253 (1997).
[48] P.-G. Reinhard, D. J. Dean, W. Nazarewicz, J. Dobaczewski, and M. R. Strayer, Phys. Rev. C (submitted).
[49] V. R. Pandharipande, C. N. Papanicolas, and J. Wambach, Phys. Rev. Lett. **53**, 1133 (1984).
[50] O. Benhar, V. R. Pandharipande, and S. C. Pieper, Rev. Mod. Phys. **65**, 817 (1993).
[51] E. Caurier, A. Poves, and A. P. Zuker, Phys. Rev. Lett. **74**, 1517 (1995).
[52] S. Raman *et al.*, At. Data Nucl. Data Tables **36**, 1 (1987).
[53] A. Poves and J. Retamosa, Phys. Lett. B **184**, 311 (1987).